EurJOC
European Journal of Organic Chemistry

Full Papers
doi.org/10.1002/ejoc.202100199

Chemistry Europe
European Chemical Societies Publishing

Special Collection

Donor-Acceptor-Donor Thienopyrazine-Based Dyes as NIR-Emitting AIEgens

Giulio Goti,*[a, b] Massimo Calamante,[a, b] Carmen Coppola,[c, d] Alessio Dessì,[a] Daniele Franchi,[a] Alessandro Mordini,*[a, b] Adalgisa Sinicropi,[a, c, d] Lorenzo Zani,[a] and Gianna Reginato[a]

Dedicated to Professor Franco Cozzi on the occasion of his 70th birthday.

Organic Near-Infrared luminophores have found broad application as functional materials, but the development of efficient NIR emitters is still a challenging goal. Here we report on a new class of thieno[3,4-*b*]pyrazine-based NIR emitting materials with Aggregation Induced Emission (AIE) properties. The dyes feature a donor–acceptor–donor (D–A–D) structure, with a thienopyrazine acceptor core connected to two triarylamine donor groups bearing a tetraphenylethylene (TPE) moiety. Fast and efficient synthesis allowed the modular preparation of three dyes of tunable absorption and emission profiles. These constructs were extensively characterized by spectroscopic studies in different solvents, which revealed intense light-harvesting ability and emissions in the deep-red and NIR region with large Stokes shift values. Remarkably, the dyes exhibited AIE properties, retaining emissive ability in the aggregate state, thus emerging as attractive materials for their potential application in the development of luminescent devices.

Introduction

Deep-red and Near-infrared (NIR) light-emitting materials have attracted increasing attention over the past few years for their use in a plethora of applications, ranging from photovoltaics, night vision, optical communication, organic light-emitting diodes (OLEDs), and bioimaging.[1] Ideal NIR emitters are able to harvest photons in the visible region with high molar attenuation coefficients (ε) and efficiently emit NIR radiation ($\lambda >$ 650 nm). Although efficient NIR emitters have been successfully developed relying both on rare-earth metals and transition metal complexes,[2] their poor availability and high costs limit their wide applicability and scalability. In this regard, purely organic NIR emitting molecules represent a valuable alternative, offering advantages in terms of ease of preparation, tunability of their photophysical properties, and reduced costs.[3]

A common strategy in designing organic NIR molecules is based on a donor-acceptor (D–A) architecture, where one (or more) strong electron-donating moiety, the donor (D), is connected to a highly electron-poor motif, the acceptor (A).[4] This approach grants access to molecules with intramolecular charge-transfer (ICT) excited state and low energy band gaps, which are ultimately responsible for the desired NIR emission. While effective, this strategy is affected by two main drawbacks: 1) as a direct consequence of the energy-gap law, radiative decay from low lying excited states is commonly associated with low emission quantum yields,[5] and 2) due to their rigid conjugated structure, D–A compounds are prone to aggregation-caused quenching (ACQ), a behavior that poses limits to their application in the solid-state.[6] Altogether, these aspects make the development of efficient organic NIR emitters challenging.

A solution to the ACQ affecting molecular dyes is provided by the aggregation-induced emission (AIE) phenomenon. Specifically, AIE luminogens (AIEgens) are molecules that, upon aggregation, exhibit enhanced emissive properties by avoiding deactivation pathways. Such AIE behavior is achieved through a combination of mechanisms, encompassing restriction of molecular motions, which also prevents deleterious π–π stacking interactions, and control of the conical intersection accessibility (CCIA).[7] During the past two decades, the deep understanding of the principles governing AIE has fostered the generation of a myriad of new AIEgens, which revealed AIE as a powerful strategy for the preparation of efficient organic NIR emitters.[8]

As part of our research interest in the synthesis and characterization of luminescent organic materials,[9] we have focused our attention on thieno[3,4-*b*]pyrazine-based dyes as

[a] Dr. G. Goti, Dr. M. Calamante, Dr. A. Dessì, Dr. D. Franchi, Dr. A. Mordini, Dr. A. Sinicropi, Dr. L. Zani, Dr. G. Reginato
Institute of Chemistry of Organometallic Compounds (ICCOM)
National Research Council (CNR)
Via Madonna del Piano 10, 50019 Sesto Fiorentino, Italy
E-mail: ggoti@iccom.cnr.it
alessandro.mordini@iccom.cnr.it
[b] Dr. G. Goti, Dr. M. Calamante, Dr. A. Mordini
Department of Chemistry "Ugo Schiff"
University of Florence
Via della Lastruccia 13,
50019 Sesto Fiorentino, Italy
[c] Dr. C. Coppola, Dr. A. Sinicropi
Department of Biotechnology, Chemistry and Pharmacy
University of Siena
Via A. Moro 2, 53100, Siena, Italy
[d] Dr. C. Coppola, Dr. A. Sinicropi
Consorzio per lo Sviluppo dei Sistemi a Grande Interfase (CSGI)
Via della Lastruccia 3,
Sesto Fiorentino, 50019, Italy

Supporting information for this article is available on the WWW under https://doi.org/10.1002/ejoc.202100199

Special Collection Part of the "Franco Cozzi's 70th Birthday" Special Collection.

potential NIR emitters. The thieno[3,4-*b*]pyrazine core is a relevant and versatile acceptor moiety in the synthesis of D–A–D molecules: *i*) its electron deficiency and poor aromaticity impart a high ICT character to the dye excited state, resulting in a deeply red-shifted absorption and emission bands; *ii*) importantly, judicious functionalization of the acceptor core enables additional tuning of the dye photophysical properties.[10] While these unique features have enabled the preparation of efficient organic NIR luminophores, the use of thieno[3,4-*b*]pyrazine in the development of NIR emitters with AIE properties has remained poorly investigated.[11]

Here we report on a new class of NIR emitting AIEgens **TP** (Scheme 1) featuring a D–A–D structure, with a thieno[3,4-*b*]pyrazine acceptor core connected to two triarylamine donor groups. Importantly, to bestow the dyes with AIE properties, we envisioned adorning the triarylamine donors with a tetraphenylethylene (TPE) moiety, whose introduction within luminophores structures is an established strategy to enhance emission from the condensed phase.[7c,8a,12] As depicted in Scheme 1, from a retrosynthetic point of view, the **TP** dyes can be obtained following a C–H functionalization logic,[10d,13] where the two C–H bonds within the acceptor core **1** are directly functionalized in the presence of an excess of the triarylamine bromide **2**. The high modularity of this approach provides straightforward access to different **TP** emitters by simple variation of the substitution pattern of acceptor **1**, which can be directly connected to the donors **2** without the need for pre-activation. Following this route, three **TP** NIR AIEgens were successfully prepared and fully characterized in solution for their photophysical and AIE properties.

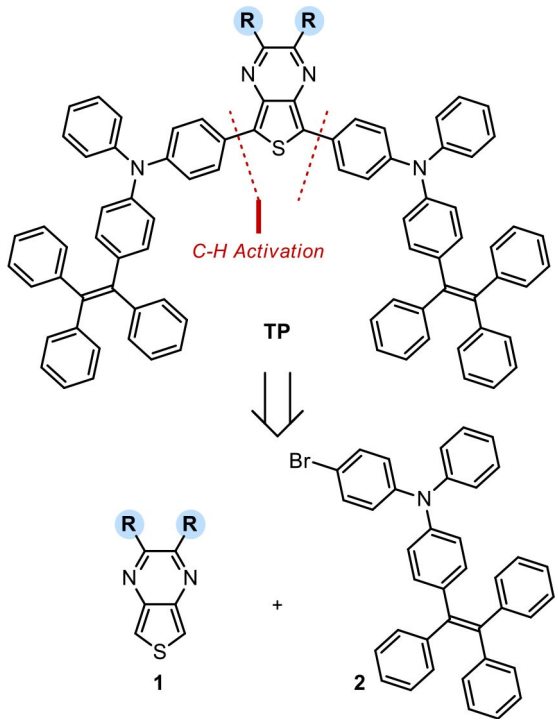

Scheme 1. Retrosynthetic analysis for **TP** emitters.

Results and Discussion

Synthesis of Compounds

Keeping in mind our retrosynthetic plan (Scheme 1), we envisaged a convergent strategy for the preparation of thieno[3,4-*b*]pyrazine dyes **TP**, where the acceptors **1** and the donor **2** are accessed through two different synthetic routes and finally assembled in a modular fashion. This synthetic strategy, depicted in Scheme 2, has allowed straightforward access to three different NIR emitters **TPa-c**. Importantly, the synthetic route strives for minimizing purification steps and is remarkable for its efficiency, both crucial aspects to be considered in view of the potential processability of the compounds.

The three thieno[3,4-*b*]pyrazine acceptor cores **1a-c** were synthesized following a reported procedure,[14] using thiophene (**3**) as an inexpensive and readily available starting material (Scheme 2a). Thiophene (**3**) was readily brominated in the presence of NBS and, after a chromatographic purification, subjected to electrophilic nitration to provide the 2,5-dibromo-3,4-dinitrothiophene **4**, which was recovered as a pure solid upon filtration (50% yield over 2 steps). Reduction of the nitro groups within **4**, along with debromination of the heteroaromatic ring, was accomplished by treatment with an excess of tin in HCl, yielding the 3,4-diaminothiophene **5**, that was isolated in gram scale upon simple filtration as a mixture of chloride and hexachlorostannate $(SnCl_6)^{2-}$ diammonium salt.[14] Finally, condensation of **5** with the 1,2-dicarbonyl compounds **6a-c** provided the three thieno[3,4-*b*]pyrazine acceptors **1a-c**. Specifically, condensation with benzil **6a** was achieved upon *in situ* deprotection of the ammonium salt **5** with an excess of triethylamine, obtaining the 2,3-diphenylthieno[3,4-*b*]pyrazine **1a** in 60% yield over two steps after chromatographic purification. The same procedure allowed the condensation of the diamine **5** with 2,3-butandione **6c** to give the 1,2-dimethyl substituted core **1c** in 81% yield over two steps, which was pure enough to be used in the next synthetic step without further manipulation. On the other hand, condensation of **5** with an excess of glyoxal **6b** occurred in basic water solution, delivering core **1b** in 79% yield over two steps with no purification needed.

The triarylamine donor **2** was synthesized starting from the commercially available bromide **7** (Scheme 2b), which was submitted to Buchwald-Hartwig coupling with aniline **8** using $Pd_2(dba)_3$ and tri-*tert*-butylphosphine as catalyst/ligand combination, furnishing the coupling product **9** in gram scale with 85% yield.[15] Following a reported procedure, the bis-arylamine **9** was then reacted with a slight excess of 1-bromo-4-iodobenzene **10** in a second C–N coupling, catalyzed by $Pd(OAc)_2$ and tri-*tert*-butylphosphine.[16] However, in our hands, these conditions led to the triarylamine product **2** only in poor yields (33%), along with the formation of a side-product (22% yield) arising from the overreaction of **2** with the starting amine **9**. To solve this issue, we conducted a short optimization (see Supporting Information, Section A), finding that an excellent balance between reactivity and selectivity is achieved using $Pd(OAc)_2$ (10 mol%) and Xantphos (15 mol%) as catalysts at

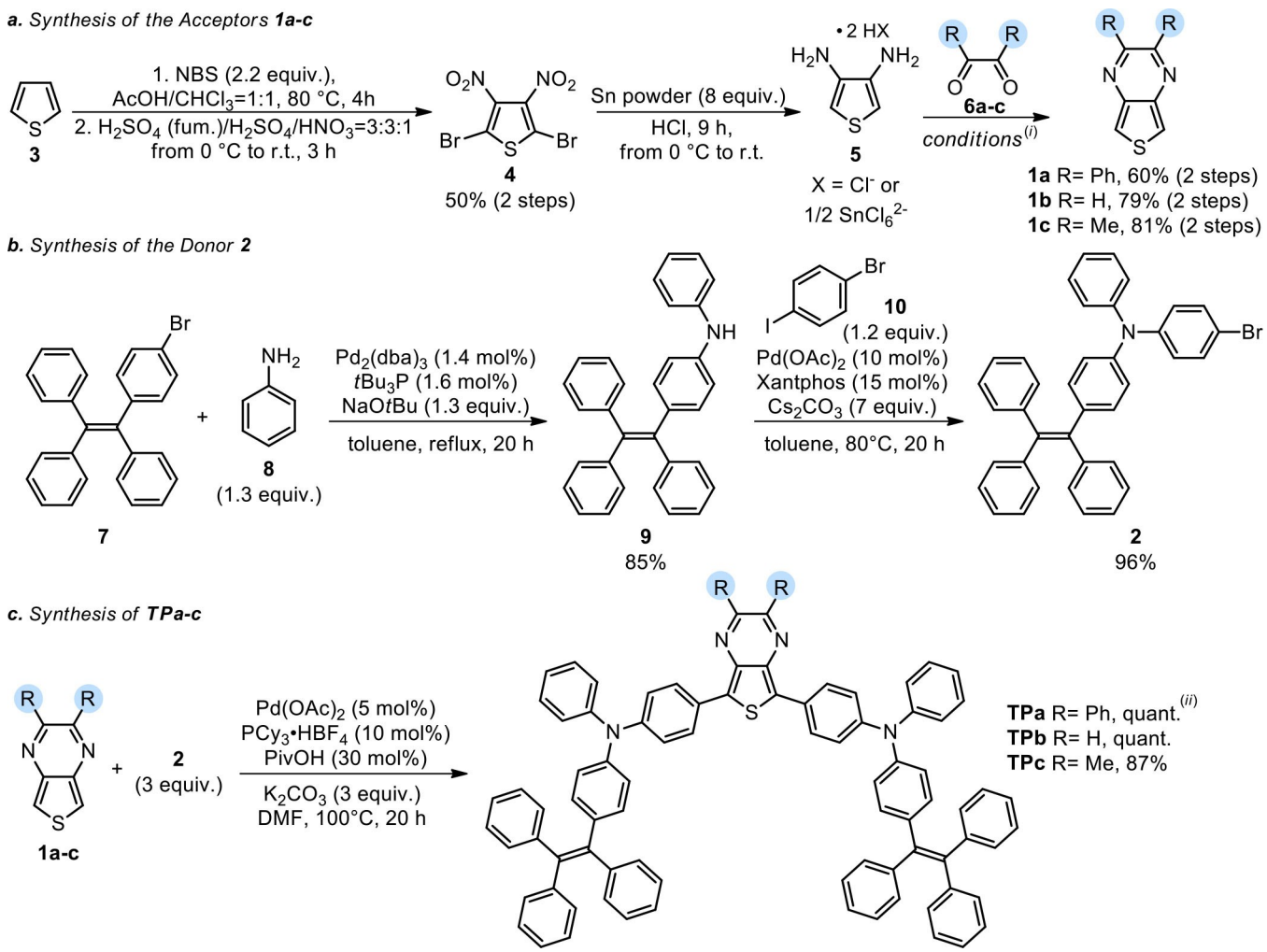

Scheme 2. Convergent synthetic route for constructs **TPa-c**. *i*) Conditions for **1a**, R = Ph: benzil **6a** (1.05 equiv.), Et_3N (4 equiv.), EtOH/DCM = 1 : 1, r.t., 3 h; for **1b**, R = H: glyoxal **6b** (40% wt in H_2O, 1.9 equiv.), H_2O, r.t., o.n.; for **1c**, R = Me: 2,3-butanedione **6c** (1 equiv.), Et_3N (4 equiv.), EtOH/DCM = 2 : 1, r.t., o.n. *ii*) Reaction time for **TPa**: 30 min. NBS = *N*-bromosuccinimide, DMF = *N*,*N*-dimethylformamide.

80 °C, which allowed the gram-scale synthesis of triarylamine **2** in 96% yield. We further found that the amount of Pd/ligand catalysts can be reduced as low as 5 mol% in palladium without loss in performance.

With all the synthons in our hands, we investigated the direct arylation of the acceptor cores **1a–c** with the donor **2** to finally obtain the targeted constructs **Tpa–c** (Scheme 2c). To our delight, arylation of both C–H bonds within the thienyl ring of cores **1a-c** occurred cleanly using $Pd(OAc)_2$ (5 mol%) and $PCy_3{\cdot}HBF_4$ (10 mol%) as a catalytic system, along with pivalic acid (30 mol%) as co-catalyst.[17] Under these conditions, we successfully synthesized the desired **Tpa–c** compounds, that were obtained after chromatographic purification with good to excellent yields (quantitative, quantitative, and 87% respectively).

Photophysical Characterization

To evaluate the ability of **Tpa–c** dyes to perform as NIR emitters, we conducted UV-Vis and emission studies to determine their photophysical properties, which are summarized below in Table 1.

Absorption spectra of **Tpa–c** solutions in dichloromethane (DCM) revealed three main absorption bands (Figure 1A): two with higher intensity in the UV region, with λ_{max} approximately centered at 310 nm and 350 nm respectively, and a third one at longer wavelengths, ascribed to the intramolecular charge transfer (ICT) transition. As it can be noted, the substitution of the thienopyrazine core strongly influences the position of the ICT absorption band. Specifically, while the non-substituted **TPb** showed an absorption maximum at 550 nm, the introduction of electron-donating methyl groups within **TPc** reduced the ICT character of the molecule, thus inducing a blue shift of the ICT band absorption maximum to 518 nm; on the contrary, a red-

Table 1. Photophysical characterization of **TPa-c** dyes in solution.

Compound	λ_{abs} [nm][a]	ε [$M^{-1}cm^{-1}$]	λ_{emi} [nm][a]	$E_{0\text{-}0}$ [eV][a]	Stokes shift [nm, eV]	Φ [%][a]	λ_{abs} [nm][b]	λ_{emi} [nm][b]	$E_{0\text{-}0}$ [eV][b]	Stokes shift [nm, eV]	Φ [%][b]
TPa	576	16876	750	1.84	174, 0.50	0.6	580	714	1.86	134, 0.40	5
TPb	550	15025	738	1.89	188, 0.57	0.3	556	703	1.92	150, 0.47	6
TPc	518	18820	679	2.02	161, 0.57	5	521	663	2.03	142, 0.51	22

[a] Measured in DCM. [b] Measured in toluene.

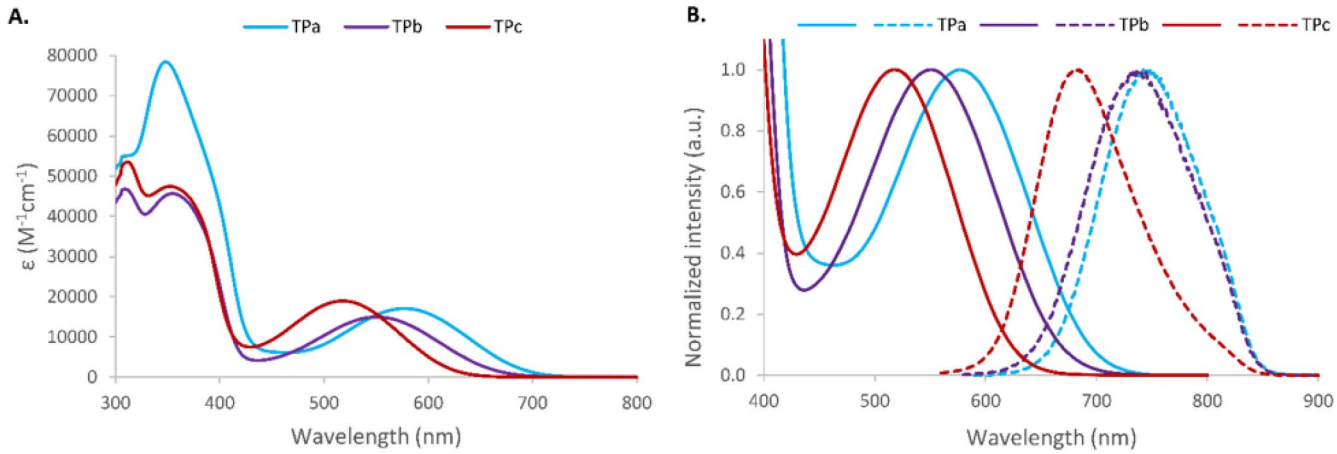

Figure 1. A) Absorption spectra of **TPa-c** solutions in DCM. B) Normalized ICT absorption bands (solid lines) and normalized emission bands (dotted lines) of **TPa-c** solutions in DCM (1×10^{-5} M, $\lambda_{exc.}$ 576 nm, 550 nm, 518 nm respectively).

shifted ICT band was observed for the highly conjugated diphenyl substituted **TPa** ($\lambda_{max}=576$ nm).

Importantly, all the **TPa-c** molecules showed deep-red to NIR emissions in DCM solution. The emission spectra (Figure 1B, dotted lines) are characterized by broad bands that mirror the corresponding ICT absorption bands well, featuring no significant vibronic structure, and considerably large Stokes shifts, >150 nm. The most blue-shifted emission in the **TP** series is observed for the dimethyl substituted **TPc** ($\lambda_{max}=679$ nm), while the emission of the diphenyl substituted **TPa** is the most red-shifted ($\lambda_{max}=750$ nm). Interestingly, the non-substituted **TPb** possesses the highest Stokes shift of the series, 188 nm (0.57 eV), thus displaying a noticeable red-shifted emission with a maximum at 738 nm.

To gain information about the influence of the solvent on the optical properties of the **TPa–c** dyes, we analyzed their absorption and emission spectra in six different media (see Supporting Information, Section D). This study showed that, while the absorption properties of **TPa–c** are only moderately affected by the nature of the solvent, the emission spectra present a marked positive solvatochromism, with maxima shifting towards longer wavelength with increasing solvent polarities. Such effect is particularly pronounced for the non-substituted **TPb**, where the emission maximum in *n*-hexane, λ_{max} 678 nm, is red-shifted by 60 nm when the solvent is changed to DCM, λ_{max} 738 nm (Figure 2A). Remarkably, a strong linear correlation between Stokes shift and the solvent polarity was observed for all **TPa–c** dyes (inset in Figure 2A for **TPb**).[18] This phenomenon is typical of push-pull organic emitters and can be ascribed to a pronounced stabilization of the highly polar charge-transfer excited states in more polar solvents. Consequently, as for the energy-gap law, narrower band-gap transitions are more susceptible to non-radiative decay, a decrease in emission intensity is observed when passing from apolar to highly polar solvents (Figure 2B). Accordingly, fluorescence quantum yields for **TPa–c** solutions in toluene, $\Phi_{Toluene}$ 5%, 6%, 22% respectively, are about one order of magnitude higher than the corresponding quantum yields measured for **TPa–c** DCM solutions, Φ_{DCM} 0.6%, 0.3%, 5% (Table 1); such quantum yield values are comparable with those of previously reported thieno[3,4-*b*]pyrazine based D–A–D emitters.[10d] Notably, the highest fluorescence quantum yield among the series of compounds is displayed by the methyl disubstituted **TPc**, as it is characterized by the highest energy band-gap.

Computational Investigation

A computational investigation based on Density Functional Theory (DFT) and time-dependent DFT (TD-DFT) methods was carried out to further rationalize the structural, electronic and photophysical properties of compounds **TPa–c**. The ground (S_0) and excited states (S_1) geometries of **TPa–c** were optimized both in DCM and in toluene and are shown in Figure S19. The S_0 optimized geometries show dihedral angles between the thieno[3,4-*b*]pyrazine acceptor core and the triarylamine donor between 10.3° and 18°, whereas calculated geometries for S_1

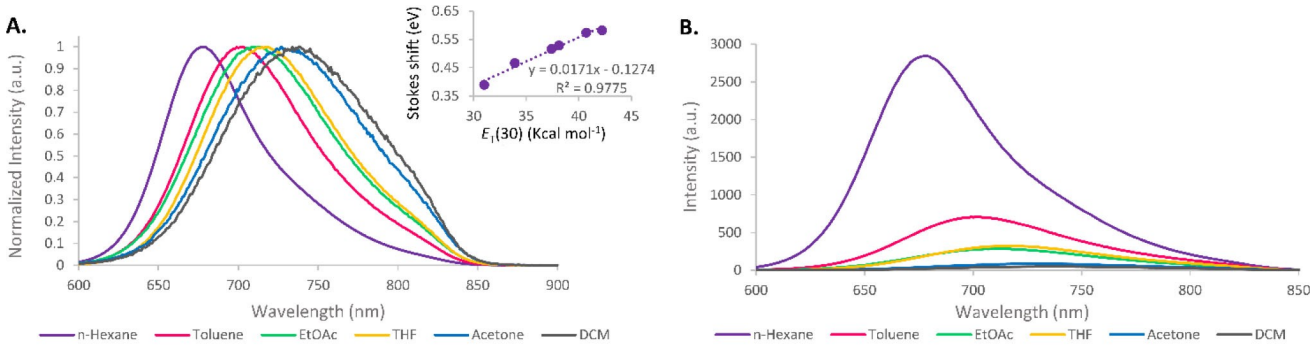

Figure 2. A) Normalized emission spectra of **TPb** solutions in different media. *Inset*: linear correlation between Stokes shift and solvent polarity. B) Variation of emission spectra intensities for **TPb** solutions (1×10^{-5} M) as a function of solvent.

show an overall increased planarity of the molecules in both solvents (dihedral angles between 0.2° and 1.2°).

TD-CAM-B3LYP/6-311 + G(2d,p) absorption (λ_{max}^{abs}) and emission (λ_{max}^{emi}) maxima, vertical excitation (E_{exc}) and emission (E_{emi}) energies, oscillator strengths (f) and composition (%) in terms of molecular orbitals for the lowest singlet-singlet excitations ($S_0 \rightarrow S_1$) and the singlet-singlet emissions ($S_1 \rightarrow S_0$) in DCM and toluene of compounds **TPa-c** are shown in Table 2 and Table 3, respectively.

TPa–c show absorption maxima in DCM between 515 and 563 nm, corresponding to 2.41-2.20 eV, while absorption maxima between 520 and 566 nm, corresponding to 2.38-2.19 eV, are calculated in toluene (Table 2). Looking at the wavefunction plot of molecular orbitals (MOs) involved in the lowest energy transitions (Figure 3), it is evident that the $S_0 \rightarrow S_1$ excitations are characterized by an intramolecular charge transfer from the donor to the acceptor group, involving HOMO→LUMO orbitals. The experimental absorption maxima are in very good agreement with the computed values in both solvents, reproducing the red-shift of the lowest energy transition going from **TPc** to **TPa**, with energy differences ≤ to 0.05 eV.

The LR-PCM computed emission maxima in DCM (Table 3) fall in the 705–769 nm range, corresponding to 1.76–1.61 eV, while emission maxima between 706–764 nm (1.76–1.62 eV) are calculated in toluene. The experimental emission maxima are also in good accordance with the computed vertical $S_1 \rightarrow S_0$ emission energies in both solvents, as the energy difference is ≤ to 0.13 eV. The calculated Stokes shifts values of **TPa–c** compounds are, respectively, 0.59, 0.63 and 0.65 eV in DCM, while 0.57, 0.60 and 0.62 eV in toluene. The wavefunction plot of molecular orbitals (MOs) involved in the lowest energy radiative transitions is shown in Figure S20 in the Supporting Information, Section F.

Table 2. TD-CAM-B3LYP/6-311 + G(2d,p) absorption maxima (λ_{max}^{abs} in nm), excitation energies (E_{exc} in eV), oscillator strengths (f) and contributions (%) to the $S_0 \rightarrow S_1$ transition in [a] DCM and [b] toluene for **TPa–c** compounds.

Compound	λ_{max}^{abs} [nm]		E_{exc} [eV]		f		Contribution [%]	
	[a]	[b]	[a]	[b]	[a]	[b]	[a]	[b]
TPa	563	566	2.20	2.19	0.71	0.71	86% H→L	89% H→L
TPb	551	556	2.25	2.23	0.81	0.80	84% H→L	85% H→L
TPc	515	520	2.41	2.38	0.95	0.93	86% H→L	86% H→L

Table 3. TD-CAM–B3LYP/6-311 + G(2d,p) emission maxima (λ_{max}^{emi} in nm), emission energies (E_{emi} in eV), oscillator strengths (f) and contributions (%) to the $S_1 \rightarrow S_0$ transition in [a] DCM and [b] toluene for **TPa–c** compounds.

Compound	λ_{max}^{emi} [nm]		E_{emi} [eV]		f		Contribution [%]	
	[a]	[b]	[a]	[b]	[a]	[b]	[a]	[b]
TPa	769	764	1.61	1.62	0.59	0.58	94% L→H	94% L→H
TPb	765	763	1.62	1.63	0.66	0.65	94% L→H	93% L→H
TPc	705	706	1.76	1.76	0.77	0.75	94% L→H	94% L→H

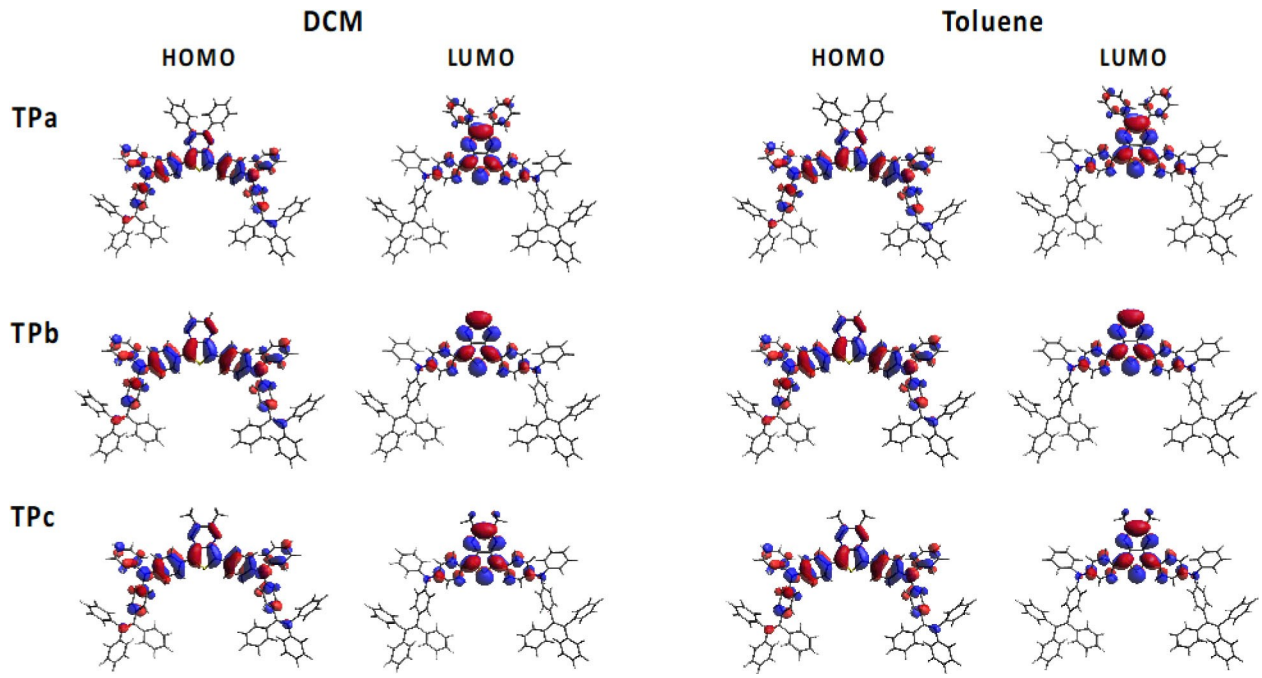

Figure 3. DFT–B3LYP/6-31G* HOMO and LUMO ground-state electron density distributions in DCM and toluene using the polarizable continuum model (PCM) of **TPa-c** compounds.

AIE Studies

The AIE properties of the **TPa-c** luminophores were investigated to assess their emission ability in the aggregated phase, an important parameter for their application as functional materials in the development of new devices. To this end, we analyzed the emission of **TPa–c** dyes in THF/water mixtures (1×10^{-5} M) with increasing water fractions, f_w (%) (Figure 4).

A moderate positive solvatochromic effect, along with a decrease in photoluminescence intensity was generally observed when going from $f_w = 0\,\%$ to $f_w = 50\,\%$ ($I/I_0 \approx 0.6$ for **TPa** and $I/I_0 \approx 0.2$ for **TPb,c**), which is likely due to an increase of the ICT character of the dyes excited state in more polar solvent mixtures. On the other hand, **TPa–c** formed soluble nanoaggregates when dissolved in solutions with $f_w \geq 60\,\%$, which induced a slight shift of emission maxima towards shorter wavelengths and an increase of photoluminescence intensity,

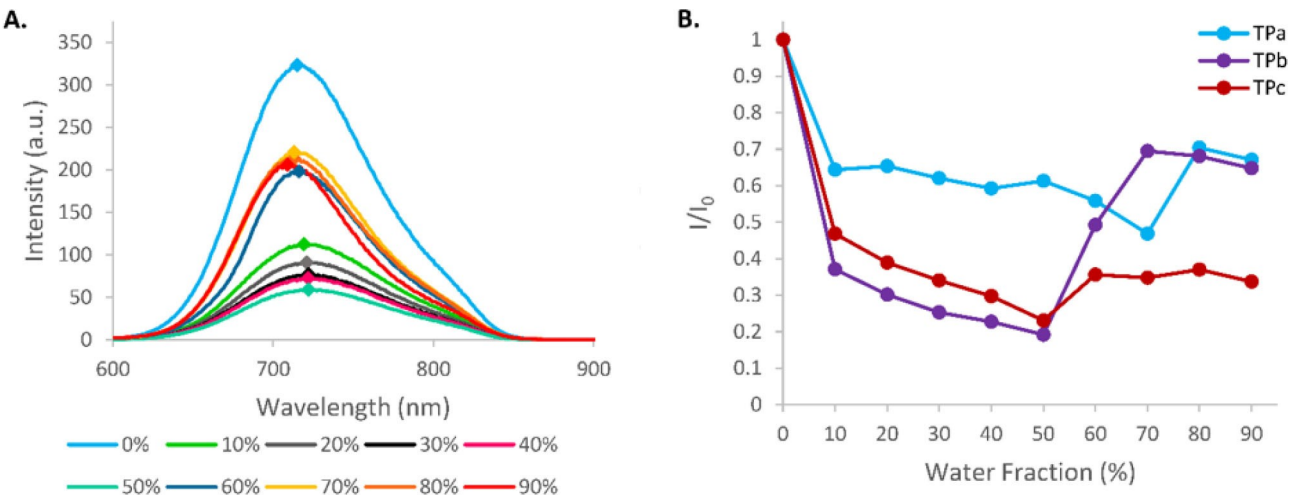

Figure 4. A) Emission spectra of **TPb** solutions in THF/water mixtures (1×10^{-5} M, $\lambda_{exc.}$ 551 nm) with increasing water fractions (%). Emission maxima are labelled as follows: ♦. B) Relative emission intensities (I/I_0) of **TPa-c** solutions in THF/water mixtures (1×10^{-5} M, $\lambda_{exc.}$ 576 nm, 551 nm, 518 nm respectively) as a function of water fraction, f_w. I and I_0 are emission intensities at the emission maximum for the compounds in THF/water mixtures ($f_w \geq 10$) and pure water ($f_w = 0$) respectively. I and I_0 values for **TPa-c** solutions have been weighted for their absorption at the excitation wavelength.

with a maximum effect at f_W of about 70%-80%. Such AIE effect was particularly marked for the **TPb** dye, with a relative intensity variation from $I/I_0 = 0.2$ to 0.7, while it was found to be less important for **TPa** and **TPc** (maximum $I/I_0 = 0.7$ and 0.37 respectively). Notably, nano-aggregates formation for **TPa–c** solutions at $f_W \geq 60\%$ was confirmed by UV-vis analysis with the onset of light scattering effects;[19] it is worth noting that such phenomenon introduces an overestimation of **TPa–c** absorbances, with consequent underestimation of the corresponding I/I_0 values.

Conclusion

In summary, we have developed new thienopyrazine based D–A–D dyes as deep-red and NIR emitters with AIE properties. A streamlined and modular synthesis enabled the straightforward assembly of three different **TPa–c** dyes with distinct photophysical properties. Importantly, all the dyes were found to strongly absorb light in the UV and visible region and to re-emit it at $\lambda_{max} > 650$ nm, with Φ values that are comparable with previously reported thienopyrazine based D–A–D luminophores. The introduction of TPE moieties within **TPa–c** structures is a key design element intended to provide the dyes with AIE properties, that were fully characterized in solution. Although moderate in some cases, an AIE effect was observed for all **TPa–c** molecules, which retained their emissive ability upon the formation of nano-aggregates in THF/water mixtures. Altogether these studies highlight thienopyrazine based D–A–D architectures as promising and versatile structures for the development of efficient NIR emitters, and will likely guide the generation of dyes with higher performances. The high processability and the advantageous photophysics of these systems suggest their potential application for the development of new emissive devices, a goal that is currently being pursued by our group.

Experimental Section

General Information

All commercially available compounds were purchased from *Merck KgaA*, *Fluorochem Ltd.*, and *T.C.I. Co. Ltd.*, and were used without further purification unless otherwise stated. Aniline **8** was distilled from KOH and stored over 4 Å molecular sieves. Anhydrous toluene, *N*,*N*-dimethylformamide (DMF), DCM, and tetrahydrofuran (THF) were obtained after drying with a PureSolv Micro apparatus (Inert). Organometallic reactions were carried out under dry nitrogen using Schlenk techniques. Reactions were monitored by TLC on Kieselgel 60 F254 (*Merck*) aluminum sheets and the products were visualized by exposing the plate to UV light or by staining it with basic aqueous potassium permanganate ($KMnO_4$) solution. Flash column chromatography[20] was performed using *Merck* Kieselgel 60 (300–400 mesh) as the stationary phase. NMR spectra were recorded on *Varian* Gemini/Mercury/INOVA instruments at 200 or 400 MHz for ^{1}H, and 50.3–100.6 MHz for ^{13}C respectively. Chemical shifts (δ) are reported in parts per million (ppm) and are referenced to the residual solvent peak ($CDCl_3$, $\delta = 7.26$ ppm for ^{1}H NMR and $\delta = 77.16$ ppm for ^{13}C NMR; THF-d_8, $\delta = 3.58$ ppm for ^{1}H NMR and $\delta = 67.21$ ppm for ^{13}C NMR; DMSO-d_6, $\delta = 2.50$ ppm for ^{1}H NMR). The following abbreviations are used to indicate the multiplicity: s, singlet; d, doublet; q, quartet; m, multiplet; bs, broad signal. GC-MS analyses were performed with a *Varian* CP-3800 gas-chromatograph coupled to a *Varian* Saturn 2200 GC/MS/MS detector and equipped with a *Varian* Chrompack Capillary Column CP-Sil 8 CB (30 m × 0.25 mm I.D. 0.25 μm df), using the following parameters: Injector temperature: 280 °C, carrier gas: He 1 mL/min, Column Temperature: 60 °C (2.5 min)–9.4 °C/min-300 °C (2 min). ESI-MS spectra were obtained by direct injection of the sample solution using a *Thermo Scientific* LCQ-FLEET instrument, while HRMS spectra were measured using a *Thermo Scientific* LTQ Orbitrap (FT-MS) instrument (carried out at the Interdepartmental Center for Mass Spectroscopy of the University of Florence, CISM); both are reported as *m/z*. UV-Vis spectra in solution were recorded with a *Varian Cary* 4000 spectrophotometer, and fluorescence spectra in solution were recorded with a *Jasco* FP-8300 spectrofluorometer, equipped with a 150 W Xenon arc lamp, irradiating the sample at the wavelength corresponding to maximum absorption in the UV spectrum (no spectral correction has been applied). Fluorescence quantum yields (Φf) in solution were measured at room temperature irradiating the sample at the wavelength corresponding to maximum absorption in the UV spectrum by means of a 152 mm diameter *Quanta-ϕ* Integrating sphere coated with *Spectralon*, that was coupled by a 1.5 m fiber optic bundle (PVC monocoil sheath, slit-round configuration, 180 fibers; slit-end termination 10 mm O.D.×50 mm long; round-end termination FR-274) to a *HORIBA Jobin-Yvon* Fluorolog-3 spectrofluorometer, equipped with a 450 W Xenon arc lamp and double-grating excitation and single-grating emission monochromator.

Synthetic Procedures

2,5-Dibromo-3,4-dinitrothiophene (4):[21] To a solution of thiophene **3** (10.0 g, 119 mmol) in a 1:1 mixture of glacial acetic acid and $CHCl_3$ (v/v) (100 mL), *N*-bromosuccinimide (46.4 g, 263 mmol) was added portion-wise and the reaction stirred vigorously at 80 °C for 4 h. Complete conversion was assessed by TLC monitoring (petroleum ether:EtOAc, 2:1), then the reaction was diluted with EtOAc (50 mL), poured in an extraction funnel, and washed with Na_2CO_3 saturated aqueous solution (2×50 mL), water (50 mL) and Brine (50 mL). The organic phase was dried over anhydrous Na_2SO_4, filtered and the solvent removed under rotatory evaporation. The crude was filtered through a pad of silica eluting with petroleum ether to get the pure 2,5-dibromothiophene as an oil (29.3 g, 90% yield). ^{1}H NMR (200 MHz, $CDCl_3$): $\delta = 6.84$ (s, 2H). Spectroscopic data are in agreement with those reported in the literature.[14] Concentrated sulfuric acid (96%, 25 mL), fuming sulfuric acid (20% SO_3, 25 mL), and concentrated nitric acid (65%, 8.3 mL) were combined in a three-neck flask equipped with a mechanical stirrer and a thermometer. The flask was cooled at 0 °C and 2,5-dibromothiophene (14.6 g, 60.2 mmol) was added maintaining the temperature below 20 °C. The reaction was stirred at room temperature for 3 h and then poured into a beaker containing 350 g of ice. Once the ice had melted, the precipitate was filtered and the solid residue extensively washed with water, obtaining 2,5-dibromo-3,4-dinitrothiophene **4** as a dark reddish solid (11.0 g, 55% yield). GC-MS (EI): $t = 18.3$ min; *m/z* (%): 161 (14), 302 (19) $[M\text{-}S]^+$, 330 (24) $[M^{79}Br^{79}Br]^+$, 332 (100) $[M^{79}Br^{81}Br]^+$, 333 (52) $[M^{81}Br^{81}Br]^+$.

3,4-Diaminothiophene salt $[\mathbf{5}{\cdot}2H^+]_x[SnCl_6^{2-}]_{(x\text{-}1/2y)}[Cl^-]_y$ **(5)**: Compound **5** was prepared by modification of a previously reported procedure.[14] 2,5-dibromo-3,4-dinitrothiophene **4** (7.9 g, 24 mmol) and concentrated HCl (37%, 40 mL) were added to a flask, the mixture was cooled to 0 °C and tin metal powder (23 g, 194 mmol)

was added portionwise. The reaction was vigorously stirred at 0 °C for 3 h, then it was allowed to reach room temperature and stirred for an additional 6 h. The mixture was cooled down in the freezer (-20 °C) to allow the formation of a precipitate, that was filtered through a fritted funnel. The solid residue was washed with cold acetonitrile (100 mL) and cold diethyl ether (100 mL), obtaining compound **5** as a pale grey solid (4.4 g). *Note*: while the corresponding free amine of derivative **5** is prone to oxidation,[22] the diammonium salt **5** is stable and could be stored in the freezer for months. ^{1}H NMR (400 MHz, DMSO-d_6): $\delta =$ 7.09 (s, 2H), 5.19 (bs, 6H). MS (ESI) *m/z*: 114.96 $[M+H]^+$. Spectroscopic data are in agreement with those reported in the literature.[14]

2,3-Diphenylthieno[3,4-*b*]pyrazine (1 a):[14] In a round bottom flask, diammonium salt **5** (500 mg, 2.67 mmol) and benzil (diphenylethanedione) **6 a** (590 mg, 2.80 mmol) were suspended in an EtOH:DCM, 1 : 1 mixture (27 mL), then triethylamine (1.50 mL, 10.7 mmol) was added and the reaction stirred at 50 °C for 5 h. Complete conversion was assessed by TLC monitoring (petroleum ether:EtOAc, 1 : 1). Water (40 mL) was added to the reaction and the mixture extracted with EtOAc (3x30 mL). The reunited organic phases were dried over anhydrous Na_2SO_4, the solution was filtered, and the solvent was evaporated under reduced pressure. The crude was purified by flash chromatography (gradient: from petroleum ether:EtOAc, 20 : 1 to 10 : 1) to give pure **1 a** as a yellow solid (464 mg, 60 % yield over 2 steps). ^{1}H NMR (400 MHz, $CDCl_3$): $\delta =$ 8.07 (s, 2H), 7.46–7.42 (m, 4H), 7.38–7.28 (m, 6H); Spectroscopic data are in agreement with those reported in the literature.[14]

Thieno[3,4-*b*]pyrazine (1 b):[14] In a round bottom flask, diammonium salt **5** (381 mg, 3.33 mmol) was dissolved in a Na_2CO_3 aqueous solution (5 % w/w, 18 mL), followed by the addition of glyoxal **6 b** (358 mg, 6.17 mmol) as a 0.65 M aqueous solution, prepared by diluting 895 mg of a 40 % wt glyoxal solution in water to 9.5 mL. The reaction was stirred at room temperature overnight, then poured in an extraction funnel and extracted with diethyl ether (7x30 mL). The reunited organic phases were dried over anhydrous Na_2SO_4, the solution was filtered, and the solvent was evaporated under reduced pressure to give crude **1 b** as a brownish solid (357 mg), which was judged pure enough to be used in the next synthetic step without further purification. ^{1}H NMR (200 MHz, $CDCl_3$): $\delta =$ 8.52 (s, 2H), 8.05 (s, 2H). Spectroscopic data are in agreement with those reported in the literature.[14]

2,3-Dimethylthieno[3,4-*b*]pyrazine (1 c):[14] In a round bottom flask, diammonium salt **5** (500 mg, 2.67 mmol) and 2,3-butanedione **6 c** (253 mg, 2.94 mmol) were suspended in a EtOH:DCM, 2 : 1 mixture (40 mL), then triethylamine (1.5 mL, 10.68 mmol) was added and the reaction stirred at 50 °C for 16 h. Water (50 mL) was added to the reaction and the mixture extracted with EtOAc (3x30 mL). The reunited organic phases were dried over anhydrous Na_2SO_4, the solution was filtered, and the solvent was evaporated under reduced pressure to give crude **1 c** as a tan solid (354 mg), which was judged pure enough to be used in the next synthetic step without further purification. ^{1}H NMR (200 MHz, $CDCl_3$): $\delta =$ 7.79 (s, 2H), 2.62 (s, 6H). Spectroscopic data are in agreement with those reported in the literature.[14]

***N*-Phenyl-4-(1,2,2-triphenylvinyl)aniline (9)**:[15] To a Schlenk tube under nitrogen atmosphere, $Pd_2(dba)_3$ (64 mg, 0.070 mmol) was added and dissolved in dry toluene (30 mL), followed by the addition of tri-*tert*-butylphosphine (20 μL, 0.080 mmol) and (2-(4-bromophenyl)ethene-1,1,2-triyl)tribenzene **7** (2.1 g, 5.0 mmol). The mixture was stirred for 10 minutes, then aniline **8** (59 μL, 6.5 mmol) and sodium *tert*-butoxide (625 mg, 6.50 mmol) were added and the reaction stirred at 120 °C for 20 h. Then the reaction was cooled down to room temperature, concentrated under reduced pressure, water (100 mL) was added and the mixture was extracted with $CHCl_3$ (3x50 mL). The organic phases were reunited and dried over anhydrous Na_2SO_4, filtered and the solvent evaporated under reduced pressure. The crude was purified by flash chromatography (gradient: from petroleum ether 90 % - DCM 10 %, to petroleum ether 85 % – DCM 15 %) to give compound **9** as a bright yellow solid (1.8 g, 85 % yield). ^{1}H NMR (400 MHz, THF-d_8): $\delta =$ 7.34 (s, 1H), 7.15 (t, $J =$ 7.7 Hz, 2H), 7.12-6.96 (m, 17H), 6.83 (d, $J =$ 8.6 Hz, 2H), 6.79 (d, $J =$ 8.8 Hz, 2H), 6.76 (t, $J =$ 7.5 Hz, 1H). ^{13}C NMR (100 MHz, THF-d_8): $\delta =$ 145.2, 145.0, 144.9, 144.1, 143.3, 141.8, 140.2, 135.7, 132.9, 132.1, 132.04, 132.01, 129.5, 128.2, 128.11, 128.11, 126.8, 126.7, 126.65, 120.7, 118.2, 116.2. MS (ESI) *m/z*: 424.18 $[M+H]^+$.

4-Bromo-*N*-phenyl-*N*-(4-(1,2,2-triphenylvinyl)phenyl)aniline (2): $Pd(OAc)_2$ (48 mg, 0.21 mmol) and Xantphos (184 mg, 0.318 mmol) were added to a Schlenk tube and put under inert atmosphere by performing three vacuum-nitrogen cycles. The solids were then dissolved in dry toluene (85 mL) and the solution was stirred for 5 minutes. Then 1-bromo-4-iodobenzene **10** (720 mg, 2.54 mmol), *N*-phenyl-4-(1,2,2-triphenylvinyl)aniline **9** (900 mg, 2.12 mmol) and caesium carbonate (4.82 g, 14.8 mmol) were added in the order and the reaction was stirred at 80 °C for 20 h. The reaction was allowed to cool down to room temperature, water (300 mL) was added, and the mixture extracted with $CHCl_3$ (3x150 mL). The organic phases were reunited and dried over anhydrous Na_2SO_4, filtered and the solvent evaporated under reduced pressure. The crude was purified by flash chromatography (gradient: from petroleum ether 98 % – DCM 2 %, to petroleum ether 90 % - DCM 10 %) to give compound **2** as a bright yellow solid (1.17 g, 96 % yield). ^{1}H NMR (400 MHz, THF-d_8): $\delta =$ 7.33 (d, $J =$ 8.9 Hz, 2H), 7.23 (t, $J =$ 7.8 Hz, 2H), 7.16–6.97 (m, 18H), 6.89 (dd, $J =$ 8.8, 2.1 Hz, 4H), 6.76 (d, $J =$ 8.6 Hz, 2H). ^{13}C NMR (100 MHz, THF-d_8): $\delta =$ 148.0, 147.8, 146.4, 144.8, 144.5, 144.2, 141.7, 141.4, 139.5, 133.0, 132.7, 131.99, 131.95, 131.93, 130.0, 128.3, 128.20, 128.19, 127.1, 127.02, 126.95, 125.9, 125.2, 124.0, 123.7, 115.3. MS (ESI) *m/z*: 577.17 $[M]^+$.

General Procedure for the synthesis of TPa-c dyes: The pyrazine derivative **1** (0.05 mmol), 4-bromo-*N*-phenyl-*N*-(4-(1,2,2-triphenylvinyl)phenyl)aniline **2** (86.8 mg, 0.150 mmol), and potassium carbonate (20.8 mg, 0.150 mmol) were added to a Schlenk tube and put under inert atmosphere by performing three vacuum-nitrogen cycles. The solids were dissolved in dry DMF (620 μL) and a solution of $Pd(OAc)_2$ (0.56 mg, 2.50 μmol), tricyclohexylphosphonium tetrafluoroborate (1.84 mg, 5.00 μmol) and pivalic acid (1.54 mg, 15.0 μmol) in DMF (100 μL) was added. Unless otherwise stated, the reaction was stirred at 100 °C for 20 h, then was allowed to cool down to room temperature, water (30 mL) was added, and the mixture extracted with $CHCl_3$ (3x10 mL). Reunited organic phases were dried over anhydrous Na_2SO_4, the solution filtered, and the solvent evaporated under reduced pressure. The crude was purified by flash chromatography to give the corresponding **TP** compound.

4,4′-(2,3-Diphenylthieno[3,4-*b*]pyrazine-5,7-diyl)bis(*N*-phenyl-*N*-(4-(1,2,2-triphenylvinyl)phenyl)aniline) (TPa): Prepared following the *general procedure* using 2,3-diphenylthieno[3,4-*b*]pyrazine **1 a** (14.4 mg, 50.0 μmol). The reaction was stirred at 100 °C for 30 minutes, then was allowed to cool down to room temperature and directly purified by flash chromatography (gradient: from petroleum ether 90 % - DCM 10 %, to petroleum ether 70 %–DCM 30 %) to give compound **TPa** as a dark blue solid (65.0 mg, quant.). ^{1}H NMR (400 MHz, THF-d_8): $\delta =$ 8.25 (d, $J =$ 8.6 Hz, 4H), 7.52 (d, $J =$ 7.1 Hz, 4H), 7.35–7.22 (m, 10H), 7.18–6.98 (m, 40H), 6.92 (d, $J =$ 8.4 Hz, 4H), 6.85 (d, $J =$ 8.5 Hz, 4H). ^{13}C NMR (100 MHz, THF-d_8; two signals are overlapped): $\delta =$ 153.0, 148.0, 147.9, 146.4, 144.8, 144.5, 144.3, 141.7, 141.5, 140.5, 139.5, 139.2, 133.0, 132.02, 131.97, 130.6, 130.5, 130.0, 129.2, 128.9, 128.6, 128.4, 128.3, 128.22, 128.21, 127.1, 127.0, 125.5, 124.1, 124.0, 123.7. HRMS (ESI): *m/z* calcd for $C_{94}H_{66}N_4S^+$: 1282.50027 $[M]^+$; found: 1282.49963.

4,4′-(Thieno[3,4-*b*]pyrazine-5,7-diyl)bis(*N*-phenyl-*N*-(4-(1,2,2-triphenylvinyl)phenyl)aniline) (TPb): Prepared following the *general procedure* using thieno[3,4-*b*]pyrazine **1b** (6.8 mg, 0.050 mmol. The crude was purified by flash chromatography (gradient: from petroleum ether 80% - DCM 20%, to petroleum ether 50% - DCM 50%) to give compound **TPb** as a light purple solid (59 mg, quant. over 3 steps). ^{1}H NMR (400 MHz, THF-d_8): $\delta = 8.47$ (d, $J = 0.7$ Hz, 2H), 8.17–8.10 (m, 4H), 7.30–7.22 (m, 4H), 7.19–6.97 (m, 40H), 6.96–6.90 (m, 4H), 6.88–6.83 (m, 4H). ^{13}C NMR (100 MHz, THF-d_8; three signals are overlapped): $\delta = 147.98$, 147.96, 146.4, 144.8, 144.5, 144.3, 141.7, 141.5, 140.7, 139.5, 133.0, 132.02, 131.97, 131.96, 131.3, 129.9, 129.1, 128.3, 128.22, 128.21, 128.1, 127.1, 126.9, 125.4, 124.0, 123.8. HRMS (ESI): *m/z* calcd for $C_{82}H_{58}N_4S^+$: 1130.43767 $[M]^+$; found: 1130.43677.

4,4′-(2,3-Dimethylthieno[3,4-*b*]pyrazine-5,7-diyl)bis(*N*-phenyl-*N*-(4-(1,2,2-triphenylvinyl)phenyl)aniline) (TPc): Prepared following the *general procedure* using 2,3-dimethylthieno[3,4-*b*]pyrazine **1c** (8.2 mg, 0.050 mmol). Respect to the *general procedure*, during the reaction work-up increased extractions from water (30 mL) with $CHCl_3$ (6x10 mL) were necessary. The crude was purified by flash chromatography (gradient: from *n*-hexane 80% - DCM 20%, to *n*-hexane 50% - DCM 50%) to give compound **TPc** as a dark red solid (50.7 mg, 70% over 3 steps). ^{1}H NMR (400 MHz, THF-d_8): $\delta = 8.16$ (d, $J = 8.8$ Hz, 4H), 7.25 (t, $J = 7.9$ Hz, 4H), 7.19–6.97 (m, 40H), 6.92 (d, $J = 8.6$ Hz, 4H), 6.85 (d, $J = 8.6$ Hz, 4H), 2.60 (s, 6H). ^{13}C NMR (100 MHz, THF-d_8): $\delta = 153.4$, 148.1, 147.5, 146.6, 144.9, 144.5, 144.3, 141.6, 141.5, 139.7, 139.3, 133.0, 132.02, 131.98, 131.97, 129.9, 129.3, 128.82, 128.81, 128.3, 128.22, 128.20, 127.04, 127.02, 126.9, 125.4, 124.0, 123.88, 123.86, 23.5. HRMS (ESI): *m/z* calcd for $C_{84}H_{62}N_4S^+$: 1158.46897 $[M]^+$; found: 1158.46826.

Computational details

Molecular and electronic properties of compounds **TPa**, **TPb**, and **TPc** have been computed via Density Functional Theory (DFT)[23,24] and Time-Dependent DFT (TDDFT)[25,26] methods, using Gaussian 16, Revision C.01 suite of programs.[27] The S_0 optimized geometries of compounds **TPa–c** have been obtained at B3LYP[28,29]/6-31G* level of theory *in vacuo*, as well as the ground-state electron density delocalization and the energy of frontier molecular orbitals (FMOs) in DCM and toluene, while the S_1 optimized geometries have been computed at TD-CAM-B3LYP[30]/6-31G* level of theory including the effects of solvent (DCM and toluene). The UV–Vis spectroscopic properties of the analyzed compounds, including absorption (λ_{max}^{abs}) and emission (λ_{max}^{emi}) maxima, vertical excitation (E_{exc}) and emission (E_{emi}) energies, oscillator strengths (f) and composition (%) in terms of molecular orbitals for the lowest singlet-singlet excitations and the singlet-singlet emissions, $S_0 \rightarrow S_1$ and $S_1 \rightarrow S_0$ respectively, in DCM and toluene, have been computed on the minimized structures at TD-CAM–B3LYP[30]/6-311+G(2d,p) level of theory. Solvent effects have been included by using the polarizable continuum model (PCM) and, in the case of the emission maxima, using the Linear-Response implementation (LR-PCM).[31]

Acknowledgements

G. G. thanks Fondazione Cassa di Risparmio di Pistoia e Pescia (Bando Giovani@Ricerca scientifica 2019, grant number 2019-0383) for a postdoctoral fellowship. We thank Prof. Andrea Pucci (University of Pisa) for performing fluorescence quantum yield measurements and the Mass Spectrometry Center (CISM) of the University of Florence for HRMS analyses.

Conflict of Interest

The authors declare no conflict of interest.

Keywords: Near-Infrared emitters · Aggregation-induced emission · Fluorescence · Functional organic materials

[1] a) H. Nakazumi, M. Matsuoka, *Chem. Rev.* **1992**, *92*, 1197–1226; b) G. Qian, Z. Y. Wang, *Chem. Asian J.* **2010**, *5*, 1006–1029; c) R. Wang, F. Zhang, *J. Mater. Chem. B* **2014**, 2, 2422–2443; d) Y. Zhang, Y. Wang, J. Song, J. Qu, B. Li, W. Zhu, W.-Y. Wong, *Adv. Opt. Mater.* **2018**, *6*, 1800466; e) F. Ding, Y. Zhan, X. Lu, Y. Sun, *Chem. Sci.* **2018**, *9*, 4370–4380; f) Q. Wei, N. Fei, A. Islam, T. Lei, L. Hong, R. Peng, X. Fan, L. Chen, P. Gao, Z. Ge, *Adv. Opt. Mater.* **2018**, *6*, 1800512.

[2] a) E. Hemmer, N. Venkatachalam, H. Hyodo, A. Hattori, Y. Ebina, H. Kishimoto, K. Soga, *Nanoscale* **2013**, *5*, 11339–11361; b) Y. Zhuang, Y. Katayama, J. Ueda, S. Tanabe, *Opt. Mater.* **2014**, *36*, 1907–1912; c) A. Barbieri, E. Bandini, F. Monti, V. K. Praveen, N. Armaroli, *Top. Curr. Chem.* **2016**, *374*, 47; d) J. Li, J. Yan, D. Wen, W. U. Khan, J. Shi, M. Wu, Q. Sua, P. A. Tanner, *J. Mater. Chem. C* **2016**, *4*, 8611–8623; e) K. T. Ly, R.-W. Chen-Cheng, H.-W. Lin, Y.-J. Shiau, S.-H. Liu, P.-T. Chou, C.-S. Tsao, Y.-C. Huang, Y. Chi, *Nat. Photonics* **2017**, *11*, 63–68.

[3] a) C.-T. Chen, *Chem. Mater.* **2004**, *16*, 4389–4400; b) Z. Sun, Q. Ye, C. Chi, J. Wu, *Chem. Soc. Rev.* **2012**, *41*, 7857–7889; c) M. Y. Wong, E. Zysman-Colman, *Adv. Mater.* **2017**, *29*, 1605444; d) Y. Liu, C. Li, Z. Ren, S. Yan, M. R. Bryce, *Nat. Rev. Mater.* **2018**, *3*, 18020; e) P. Data, Y. Takeda, *Chem. Asian J.* **2019**, *14*, 1613–1636; f) A. Zampetti, A. Minotto, F. Cacialli, *Adv. Funct. Mater.* **2019**, *29*, 1807623; g) Y. Xu, P. Xu, D. Hu, Y. Ma, *Chem. Soc. Rev.* **2021**, ***50***, 1030–1069; h) B. Li, M. Zhao, F. Zhang, *ACS Materials Lett.* **2020**, *2*, 905–917; i) S. Liu, Y. Li, R. T. K. Kwok, J. W. Y. Lama, B. Z. Tang, *Chem. Sci.* **2021**, DOI: 10.1039/d0sc02911d.

[4] a) K. Umezawa, Y. Nakamura, H. Makino, D. Citterio, K. Suzuki, *J. Am. Chem. Soc.* **2008**, *130*, 1550–1551; b) T. Weil, T. Vosch, J. Hofkens, K. Peneva, K. Müllen, *Angew. Chem. Int. Ed.* **2010**, *49*, 9068–9093; *Angew. Chem.* **2010**, *122*, 9252–9278; c) H. Bürckstümmer, A. Weissenstein, D. Bialas, F. Würthner, *J. Org. Chem.* **2011**, *76*, 2426–2432; d) U. Mayerhöffer, B. Fimmel, F. Würthner, *Angew. Chem. Int. Ed.* **2012**, *51*, 164–167; *Angew. Chem.* **2012**, *124*, 168–171; e) Y. Koide, Y. Urano, K. Hanaoka, W. Piao, M. Kusakabe, N. Saito, T. Terai, T. Okabe, T. Nagano, *J. Am. Chem. Soc.* **2012**, *134*, 5029–5031; f) M. Shimizu, R. Kaki, Y. Takeda, T. Hiyama, N. Nagai, H. Yamagishi, H. Furutani, *Angew. Chem. Int. Ed.* **2012**, *51*, 4095–4099; *Angew. Chem.* **2012**, *124*, 4171–4175; g) L. Yao, S. Zhang, R. Wang, W. Li, F. Shen, B. Yang, Y. Ma, *Angew. Chem. Int. Ed.* **2014**, *53*, 2119–2123; *Angew. Chem.* **2014**, *126*, 2151–2155; h) Y. Yuan, Y. Hu, Y.-X. Zhang, J.-D. Lin, Y.-K. Wang, Z.-Q. Jiang, L.-S. Liao, S.-T. Lee, *Adv. Funct. Mater.* **2017**, *27*, 1700986; i) C. Li, R. Duan, B. Liang, G. Han, S. Wang, K. Ye, Y. Liu, Y. Yi, Y. Wang, *Angew. Chem. Int. Ed.* **2017**, *56*,11525–11529; *Angew. Chem.* **2017**, *129*, 11683–11687; j) D.-H. Kim, A. D'Aléo, X.-K. Chen, A. D. S. Sandanayaka, D. Yao, L. Zhao, T. Komino, E. Zaborova, G. Canard, Y. Tsuchiya, E. Choi, J. W. Wu, F. Fages, J.-L. Brédas, J.-C Ribierre, C. Adachi, *Nat. Photonics* **2018**, *12*, 98–104; k) S. Wang, J. Liu, C. C. Goh, L. G. Ng, B. Liu, *Adv. Mater.* **2019**, *31*, 1904447; l) C. Lv, W. Liu, Q. Luo, H. Yi, H. Yu, Z. Yang, B. Zou, Y. Zhang, *Chem. Sci.* **2020**, *11*, 4007–4015.

[5] a) W. Siebrand, *J. Chem. Phys.* **1967**, *46*, 440–447; b) J. V. Caspar, E. M. Kober, B. P. Sullivan, T. J. Meyer, *J. Am. Chem. Soc.* **1982**, *104*, 630–632.

[6] a) Y. Huang, J. Xing, Q. Gong, L.-C. Chen, G. Liu, C. Yao, Z. Wang, H.-L. Zhang, Z. Chen, Q. Zhang, *Nat. Commun.* **2019**, *10*, 169; b) K. Zhang, J. Liu, Y. Zhang, J. Fan, C.-K. Wang, L. Lin, *J. Phys. Chem. C* **2019**, *123*, 24705–24713.

[7] a) J. Luo, Z. Xie, J. W. Y. Lam, L. Cheng, H. Chen, C. Qiu, H. S. Kwok, X. Zhan, Y. Liu, D. Zhuc, B. Z. Tang, *Chem. Commun.* **2001**, 1740–1741; b) J. Mei, Y. Hong, J. W. Y. Lam, A. Qin, Y. Tang, B. Z. Tang, *Adv. Mater.* **2014**, *26*, 5429–5479; c) J. Mei, N. L. C. Leung, R. T. K. Kwok, J. W. Y. Lam, B. Z. Tang, *Chem. Rev.* **2015**, *115*, 11718–11940; d) K. Kokado, K. Sada, *Angew. Chem. Int. Ed.* **2019**, *58*, 8632–8639; *Angew. Chem.* **2019**, *131*, 8724–8731; e) S. Suzuki, S. Sasaki, A. S. Sairi, R. Iwai, B. Z. Tang, G. Konishi, *Angew. Chem. Int. Ed.* **2020**, *59*, 9856–9867; *Angew. Chem.* **2020**, *132*, 9940–9951.

[8] a) Q. Zhao, J. Z. Sun, *J. Mater. Chem. C* **2016**, *4*, 10588–10609; b) W. Xu, D. Wang, B. Z. Tang, *Angew. Chem. Int. Ed.* **2020**, DOI:10.1002/anie.202005899.
[9] a) C. Papucci, T. A. Geervliet, D. Franchi, O. Bettucci, A. Mordini, G. Reginato, F. Picchioni, A. Pucci, M. Calamante, L. Zani, *Eur. J. Org. Chem.* **2018**, 2657–2666; b) A. Dessì, M. Bartolini, M. Calamante, L. Zani, A. Mordini, G. Reginato, *Synthesis* **2018**, *50*, 1284–1292; c) C. Papucci, A. Dessì, C. Coppola, A. Sinicropi, G. Santi, M. Di Donato, M. Taddei, P. Foggi, L. Zani, G. Reginato, A. Pucci, M. Calamante, A. Mordini, *Dyes Pigm.* **2021**, *188*, 109207.
[10] a) S. C. Rasmussen, R. L. Schwiderski, M. E. Mulholland, *Chem. Commun.* **2011**, *47*, 11394–11410; b) R. L. Schwiderski, S. C. Rasmussen, *J. Org. Chem.* **2013**, *78*, 5453–5462; c) X. Lu, S. Fan, J. Wu, X. Jia, Z.-S. Wang, G. Zhou, *J. Org. Chem.* **2014**, *79*, 6480–6489; d) L. E. McNamara, N. Liyanage, A. Peddapuram, J. S. Murphy, J. H. Delcamp, N. I. Hammer, *J. Org. Chem.* **2016**, *81*, 32–42.
[11] J. Qi, X. Duan, Y. Cai, S. Jia, C. Chen, Z. Zhao, Y. Li, H.-Q. Peng, R. T. K. Kwok, J. W. Y. Lam, D. Ding, B. Z. Tang, *Chem. Sci.* **2020**, *11*, 8438–8447.
[12] a) W. Qin, K. Li, G. Feng, M. Li, Z. Yang, B. Liu, B. Z. Tang, *Adv. Funct. Mater.* **2014**, *24*, 635–643; b) Z. Sheng, B. Guo, D. Hu, S. Xu, W. Wu, W. H. Liew, K. Yao, J. Jiang, C. Liu, H. Zheng, B. Liu, *Adv. Mater.* **2018**, *30*, 1800766.
[13] a) N. P. Liyanage, A. Yella, M. Nazeeruddin, M. Grätzel, J. H. Delcamp, *ACS Appl. Mater. Interfaces* **2016**, *8*, 5376–5384; b) N. P. Liyanage, H. Cheema, A. R. Baumann, A. R. Zylstra, J. H. Delcamp, *ChemSusChem* **2017**, *10*, 2635–2641; Selected reviews on C–H activation:; c) X. Chen, K. M. Engle, D.-H. Wang, J.-Q. Yu, *Angew. Chem. Int. Ed.* **2009**, *48*, 5094–5115; *Angew. Chem.* **2009**, *121*, 5196–5217; d) J. Wencel-Delord, F. Glorius, *Nat. Chem.* **2013**, *5*, 369–375.
[14] D. D. Kenning, K. A. Mitchell, T. R. Calhoun, M. R. Funfar, D. J. Sattler, S. C. Rasmussen, *J. Org. Chem.* **2002**, *67*, 9073–9076.
[15] K. Li, W. Qin, D. Ding, N. Tomczak, J. Geng, R. Liu, J. Liu, X. Zhang, H. Liu, B. Liu, B. Z. Tang, *Sci. Rep.* **2013**, *3*, 1150.
[16] T. Jiang, Y. Qu, B. Li, Y. Gao, J. Hua, *RSC Adv.* **2015**, *5*, 1500–1506.
[17] a) S. I. Gorelsky, D. Lapointe, K. Fagnou, *J. Am. Chem. Soc.* **2008**, *130*, 10848–10849; b) B. Liégault, D. Lapointe, L. Caron, A. Vlassova, K. Fagnou, *J. Org. Chem.* **2009**, *74*, 1826–1834.
[18] C. Reichardt, *Chem. Rev.* **1994**, *94*, 2319–2358.
[19] a) A. Qin, L. Tang, J. W. Y. Lam, C. K. W. Jim, Y. Yu, H. Zhao, J. Sun, B. Z. Tang, *Adv. Funct. Mater.* **2009**,*19*,1891–1900; b) M. P. Aldred, C. Li, M.-Q. Zhu, *Chem. Eur. J.* **2012**, *18*, 16037–16045; c) S. Sasaki, Y. Niko, K. Igawa, G. Konishi, *RSC Adv.* **2014**, *4*, 33474–33477.
[20] W. C. Still, M. Kahn, A. Mitra, *J. Org. Chem.* **1978**, *43*, 2923–2925.
[21] The procedure for the bromination reaction to give 2,5-dibromothiophene was adapted from: a) R. M. Kellogg, A. P. Schaap, E. T. Harper, H. Wynberg, *J. Org. Chem.* **1968**, *33*, 29022909; the procedure for the nitration reaction to give **4** was adapted from: b) L. Wen, S. C. Rasmussen, *J. Chem. Crystallogr.* **2007**, *37*, 387–398.
[22] N. I. Abdo, A. A. El-Shehawy, A. A. El-Barbary, J.-S. Lee, *Eur. J. Org. Chem.* **2012**, 5540–5551.
[23] P. Hohenberg, W. Kohn, *Phys. Rev.* **1964**, *136*, B864-B871.
[24] W. Kohn, L. J. Sham, *Phys. Rev.* **1965**, *140*, A1134-A1138.
[25] C. Adamo, D. Jacquemin, *Chem. Soc. Rev.* **2013**, *42*, 845–856.
[26] A. D. Laurent, C. Adamo, D. Jacquemin, *Phys. Chem. Chem. Phys.* **2014**, *16*, 14334–14356.
[27] Gaussian 16, Revision C.01, M. J. Frisch, G. W. Trucks, H. B. Schlegel, G. E. Scuseria, M. A. Robb, J. R. Cheeseman, G. Scalmani, V. Barone, G. A. Petersson, H. Nakatsuji, X. Li, M. Caricato, A. V. Marenich, J. Bloino, B. G. Janesko, R. Gomperts, B. Mennucci, H. P. Hratchian, J. V. Ortiz, A. F. Izmaylov, J. L. Sonnenberg, D. Williams-Young, F. Ding, F. Lipparini, F. Egidi, J. Goings, B. Peng, A. Petrone, T. Henderson, D. Ranasinghe, V. G. Zakrzewski, J. Gao, N. Rega, G. Zheng, W. Liang, M. Hada, M. Ehara, K. Toyota, R. Fukuda, J. Hasegawa, M. Ishida, T. Nakajima, Y. Honda, O. Kitao, H. Nakai, T. Vreven, K. Throssell, J. A. Montgomery, Jr., J. E. Peralta, F. Ogliaro, M. J. Bearpark, J. J. Heyd, E. N. Brothers, K. N. Kudin, V. N. Staroverov, T. A. Keith, R. Kobayashi, J. Normand, K. Raghavachari, A. P. Rendell, J. C. Burant, S. S. Iyengar, J. Tomasi, M. Cossi, J. M. Millam, M. Klene, C. Adamo, R. Cammi, J. W. Ochterski, R. L. Martin, K. Morokuma, O. Farkas, J. B. Foresman, and D. J. Fox, Gaussian, Inc., Wallingford CT, **2016**.
[28] A. D. Becke, *J. Chem. Phys.* **1993**, *98*, 5648–5652.
[29] C. Lee, W. Yang, R. G. Parr, *Phys. Rev. B.* **1988**, *37*, 785–789.
[30] T. Yanai, D. P. Tew, N. C. Handy, *Chem. Phys. Lett.* **2004**, *393*, 51–57.
[31] J. Tomasi, B. Mennucci, R. Cammi, *Chem. Rev.* **2005**, *105*, 2999–3094.

Manuscript received: February 18, 2021
Revised manuscript received: March 22, 2021
Accepted manuscript online: March 29, 2021